Flat-top and patterned-topped cone gratings for visible and mid-infrared antireflective properties

Jean-Baptiste Brueckner, Judikaël Le Rouzo, Ludovic Escoubas, Gerard Berginc, Cecile Gourgon, Olivier Desplats, Jean-Jacques Simon

Flat-top and patterned-topped cone gratings for visible and mid-infrared antireflective properties

Jean-Baptiste Brückner,[1,*] Judikaël Le Rouzo,[1] Ludovic Escoubas,[1] Gérard Berginc,[2] Cécile Gourgon,[3] Olivier Desplats,[3] and Jean-Jacques Simon[1]

[1]*Aix-Marseille Université, Institut Matériaux Microélectronique Nanosciences de Provence - IM2NP, CNRS-UMR 6242, Domaine Universitaire de Saint-Jérôme, Service 231, 13397 Marseille Cedex20, France*
[2]*THALES Optronique SA, 2 Avenue Gay Lussac, Elancourt, France*
[3]*Lab. des Technologies de la Microélectronique, LTM CNRS-UMR 5129, 17 Avenue des Martyrs, 38054 Grenoble, France*
[*]*jean-baptiste.bruckner@im2np.fr*

Abstract: Achieving a broadband antireflection property from material surfaces is one of the highest priorities for those who want to improve the efficiency of solar cells or the sensitivity of photo-detectors. To lower the reflectance of a surface, we are concerned with the study of the optical response of flat-top and patterned-topped cone shaped silicon gratings, based on previous work exploring pyramid gratings. Through rigorous numerical methods such as Finite Different Time Domain, we first designed several flat-top structures that theoretically demonstrate an antireflective character within the middle infrared region. From the opto-geometrical parameters such as period, depth and shape of the pattern determined by numerical analysis, these structures have been fabricated using controlled slope plasma etching processes. In order to extend the antireflective properties up to the visible wavelengths, patterned-topped cones have been fabricated as well. Afterwards, optical characterizations of several samples were carried out. Thus, the performances of the flat-top and patterned-topped cones have been compared in the visible and mid infrared range.

OCIS codes: (050.1950) Diffraction gratings; (310.1210) Antireflection coatings.

References and links

1. S. Chattopadhyay, Y. F. Huang, Y. J. Jen, A. Ganguly, K. H. Chen, and L. C. Chen, "Anti-reflecting and photonic nanostructures," Mater. Sci. Engineering: R: Reports **69**(1-3), 1–35 (2010).
2. K. M. Baker, "Highly corrected close-packed microlens arrays and moth-eye structuring on curved surfaces," Appl. Opt. **38**(2), 352–356 (1999).
3. D. M. Braun, "Design of single layer antireflection coatings for InP/$In_{0.53}Ga_{0.47}As$/InP photodetectors for the 1200-1600-nm wavelength range," Appl. Opt. **27**(10), 2006–2011 (1988).
4. K. T. Park, Z. Guo, H. D. Um, J. Y. Jung, J. M. Yang, S. K. Lim, Y. S. Kim, and J. H. Lee, "Optical properties of Si microwires combined with nanoneedles for flexible thin film photovoltaics," Opt. Express **19**(S1 Suppl 1), A41–A50 (2011).
5. N. Yamada, T. Ijiro, E. Okamoto, K. Hayashi, and H. Masuda, "Characterization of antireflection moth-eye film on crystalline silicon photovoltaic module," Opt. Express **19**(S2 Suppl 2), A118–A125 (2011).
6. J. Oh, H. C. Yuan, and H. M. Branz, "An 18.2%-efficient black-silicon solar cell achieved through control of carrier recombination in nanostructures," Nat. Nanotechnol. **7**(11), 743–748 (2012).
7. K. Forberich, G. Dennler, M. C. Scharber, K. Hingerl, T. Fromherz, and C. J. Brabec, "Performance improvement of organic solar cells with moth eye anti-reflection coating," Thin Solid Films **516**(20), 7167–7170 (2008).
8. H. A. MacLeod, *Thin-Film Optical Filters* (Taylor & Francis Ed. IV, (2010) p. 668.
9. P. B. Clapham and M. C. Hutley, "Reduction of lens reflection by the 'moth eye' principle," Nature **244**(5414), 281–282 (1973).
10. M. Born and E. Wolf, in *Principle of Optics* (Pergamon, 1980) pp. 705–708.
11. E. Grann, M. G. Varga, and D. Pommet, "Optimal design for antireflective tapered two dimensional subwavelength grating structures," J. Opt. Soc. Am. A **12**(2), 333–339 (1995).

#190203 - $15.00 USD Received 8 May 2013; revised 15 Jun 2013; accepted 24 Jun 2013; published 27 Jun 2013

12. S. K. Srivastava, D. Kumar, K. Singh, M. Kar, V. Kumar, and M. Husain, "Excellent antireflection properties of vertical nanowire arrays," Sol. Energy Mater. Sol. Cells **94**(9), 1506–1511 (2010).
13. J. Zhou, M. Hildebrandt, and M. Lu, "Self-organized antireflecting nano-cone arrays on Si (100) induced by ion bombardment," J. Appl. Phys. **109**(5), 053513 (2011).
14. H. Yuan, V. E. Yost, M. R. Page, P. Stradins, D. L. Meier, and H. M. Branz, "Efficient black silicon solar cell with a density-graded nanoporous surface: Optical properties, performance limitations, and design rules," Appl. Phys. Lett. **95**(12), 123501 (2009).
15. L. Escoubas, J. J. Simon, M. Loli, G. Berginc, F. Flory, and H. Giovannini, "An antireflective silicon grating working in the resonance domain for near infrared spectral region," Opt. Commun. **226**(1-6), 81–88 (2003).
16. R. Bouffaron, L. Escoubas, J. J. Simon, P. Torchio, F. Flory, G. Berginc, and P. Masclet, "Enhanced antireflecting properties of microstructured flat-top pyramids," J. Opt. Soc. Am. A **16**, 19304–19309 (2008).
17. L. Escoubas, R. Bouffaron, V. Brissonneau, J. J. Simon, G. Berginc, F. Flory, and P. Torchio, "Sand-castle biperiodic pattern for spectral and angular broadening of antireflective properties," Opt. Lett. **35**(9), 1455–1457 (2010).
18. M. G. Moharam, E. B. Grann, D. A. Pommet, and T. K. Gaylord, "Formulation for stable and efficient implementation of the rigorous coupled wave analysis of binary gratings," J. Opt. Soc. Am. A **12**(5), 1068–1076 (1995).
19. E. D. Palik, in *Handbook of Optical Constants*, (Academic Press, 555–568, 1985, I).
20. Y. F. Huang, S. Chattopadhyay, Y. J. Jen, C. Y. Peng, T. A. Liu, Y. K. Hsu, C. L. Pan, H. C. Lo, C. H. Hsu, Y. H. Chang, C. S. Lee, K. H. Chen, and L. C. Chen, "Improved broadband and quasi-omnidirectional anti-reflection properties with biomimetic silicon nanostructures," Nat. Nanotechnol. **2**(12), 770–774 (2007).

1. Introduction

Over the last few years, antireflective gratings have been widely investigated with the emergence of photovoltaics and photosensing. Reducing the reflection losses from incident radiation has become one of the highest priorities for such devices. Controlling the reflection of incident radiation over an interface has then offered numerous applications for a wide range of domains [1]. For instance, optical systems such as lenses need an antireflective treatment to maximize their transmission coefficient [2]. For a photodetector, reducing reflection is an important matter, since the better the light penetrates into the material, the more it improves its response [3]. In photovoltaics, solar cells treated with an antireflective coating see their photon to electron conversion rate increased. Therefore, with the help of antireflective (AR) coatings, the efficiency of these devices has been greatly enhanced over the last few years [4–7]. Concerning the stealth domain, reducing the optical signature of a surface is an important matter as well.

It is possible to distinguish different kinds of antireflective coatings. In the first place there are optical thin films with controlled refractive indices and thicknesses, widely used over time to achieve low reflectivity over a large and tunable band of wavelength [8]. Nonetheless, for some applications, thicknesses of such coating are critical parameters and thus many other ways to reduce reflection have been investigated. Following the observation of small conical microstructures with antireflective properties on the surface of the eye of a moth that provide the insect a better night vision [9], many works have been carried out on structured surfaces. The Effective Medium Theory has then been developed, explaining low reflectivity by the gradual change in indices occurring in theses sub-wavelength structures [10,11]. The arrangement, sizes and shapes of these structures have a fundamental influence on the optical response. Random structuration at the surface of a silicon substrate and in the form of nanowires [12] or nanocones [13] of different size and shape also offer a strong and large antireflective band. Reflectivity is generally less than 1% in the visible range, giving a deep black aspect of the surface. Therefore the structure received the name of the black silicon [14]. A major drawback of the randomized structures is that computation requires enormous amount of memory in order to predict their optical properties. On the other hand, periodic structures allow a more tunable antireflective band and their optical properties are easy to compute through electromagnetic analysis. However, they are slightly less effective in terms of antireflective efficiency than the former ones [15]. The principle objective here is to design an antireflective grating demonstrating a low reflection coefficient in specified spectral bands (the 0.7-2.5 and 3-5 μm regions). Therefore 2D periodic silicon gratings have been

#190203 - $15.00 USD Received 8 May 2013; revised 15 Jun 2013; accepted 24 Jun 2013; published 27 Jun 2013

investigated. Previous works theoretically showed that silicon flat-top pyramid gratings could demonstrate a low reflection coefficient in the 3-5 µm region [16]. It has been demonstrated as well that adding a second periodicity level by patterning the top flat pyramid allows theoretically to extend the antireflective band down to the 0.7-2.5 µm region [17]. This idea came from the fact that those structures have a constant behavior when a scale factor (multiplying all the geometrical dimensions with the same value) is applied. To fabricate the flat-top and patterned-topped pyramids, plasma etching on silicon is preferred. Thus, according to the elaboration technique limits, numerical analyses are performed in order to set a realistic range of geometric parameters depicted in Fig. 1. Another constraint has to be added to the gratings. As for every diffraction grating, depending on the wavelength of the incident radiation, diffracted orders may appear and could lead to cross talking effects that are undesirable, for instance, to pixels of CMOS or CCD optical sensors. Thus, in order to determine the diffracted order efficiencies appearing on both pyramid structures, Fourier Modal Method (FMM) analysis has been performed as well [18]. Unfortunately, the plasma etching fabrication could not allow for making a straight pyramid shape. Therefore cone gratings have been carried out instead. Nonetheless, optical specifications are kept the same. Thereafter, FTIR measurements have then been performed in order to determine the efficiency of the fabricated samples. Finally, performances of the patterned-topped cone gratings have been compared with the flat-topped ones.

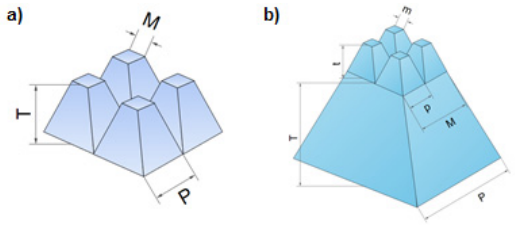

Fig. 1. Schematic view and geometric parameters of the flat-top (a) and patterned-topped (b) pyramids. P is the period, T the thickness and M the flat-top's length. Concerning the patterned-topped structure, m, p and t are the parameters of the second periodicity level.

2. Numerical analysis

2.1 Computational tools

The parametric study has been performed through Finite Difference Time Domain Method (FDTD) with FullWave, a commercial software. Based on spatial and temporal discretization of Maxwell's equations, the FDTD method is commonly used to solve the propagation of electromagnetic waves in complex structures. The computation requires a geometry definition of the structure and refractive indices of materials n (λ) and k (λ) taken from the Palik [19] database. Continuous and monochromatic waves are used to determine the optical behavior. The simulation space is described by a domain discretized by a uniform mesh where, for each of its nodes, the electric and magnetic components of the field are calculated. The adjustment of the mesh is very important as if it is too narrow, computation time becomes too long. Moreover, if it is too coarse, the risk of not taking into account all physical phenomena present, which can greatly distort the results. Thus, after various convergence tests, a 10 nm mesh along the x, y and z directions was sufficient to offer acceptable results with the smallest calculation time. As for the time step, it is defined to be smaller than the propagation time of the wave between two nodes. Concerning the boundary conditions, periodic conditions are used to repeat periodically the defined pattern along the x and y axis, allowing the simulations of the interactions with neighboring structures, and a "Perfectly Matched Layer" is set on the top and bottom of the computational domain, simulating a highly absorbent material as depicted by Fig. 2. Thus, only a negligible energy would be reflected back in this domain. In order to investigate the diffraction order efficiencies, calculations by Fourier Modal Method

#190203 - $15.00 USD Received 8 May 2013; revised 15 Jun 2013; accepted 24 Jun 2013; published 27 Jun 2013

with the commercial software VirtualLab from Lighttrans have been used. This rigorous solving method is commonly used for solving electromagnetism problems in diffraction gratings. It is mainly based on the decomposition of the structure into 10 nm layers, allowing the decomposition of the permittivity into Fourier series. The decomposed permittivity is then injected into the Maxwell's equations. Thus, reflection and transmission coefficients are determined, as well as the efficiencies associated to each diffracted order.

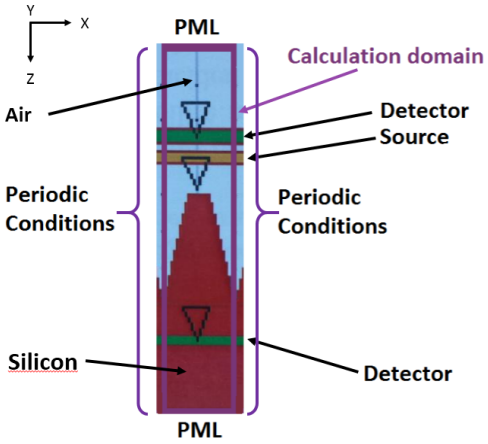

Fig. 2. Schematic of the unit cell for the FDTD calculation and the corresponding boundary conditions.

2.2 Determination of critical parameters and parametric study

The flat-top pyramid is periodically repeated along x and y spatial axes. The period P, the thickness T, the length of the flat-top M and the spacing between the structures s are the pattern's parameters. This grating can achieve a reflectivity less than 2% for the 3-5 µm region [11]. The angle of the pyramid slope θ is a function of the geometric parameters:

$$\theta = \arctan\left(\frac{2T}{P-M}\right). \quad (1)$$

As the antireflective properties are given by the gradual change of index between the freespace and the silicon, the angle θ and thus the geometric parameters of the pyramid have a strong influence on the grating's efficiency. Even though the plasma etching is an accurate fabrication technique, most of the samples will not present exactly the same parameters. Therefore, through FDTD and Modal Fourier Method calculations, a set of parameters permitting to achieve an acceptable antireflective grating in the 3-5 µm region has been studied and is discussed in the next sections. The reference structure has the following parameters: P = 1 µm, T = 1.5 µm, M = 0.375 µm and s = 0 µm and θ = 78.7 °.

2.2.1 Diffracted orders

A critical constraint has to be added to the antireflective grating. No diffracted order may be present in the air, and we have to limit those present in the substrate as much as possible, in order to avoid cross talking situations in the case of imaging sensors such as CCD or CMOS sensors. For recall, a wave encountering a grating of period P with an incident angle θ_i is diffracted in transmission and in reflection, into a certain number of orders (Fig. 3).

#190203 - $15.00 USD Received 8 May 2013; revised 15 Jun 2013; accepted 24 Jun 2013; published 27 Jun 2013

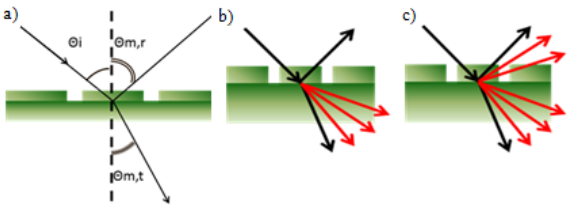

Fig. 3. Illustration of a diffraction grating without any orders (a), with orders in the substrate only (b), and with transmitted and reflected orders (c).

As described in the works of Bouffaron [16], for a given wavelength λ, the condition to avoid any diffracted orders in the incident medium of index n_i or in the substrate of index n_s, is the following one:

$$P \le \frac{\lambda}{n_s + n_i \sin\theta_i}. \tag{2}$$

When going a little further, condition for the existence of diffracted orders in the substrate only, may be written as following:

$$\frac{\lambda}{n_s + n_i \sin\theta_i} \le P \le \frac{\lambda}{n_i + n_i \sin\theta_i}. \tag{3}$$

And finally, both transmitted and reflected orders are present for:

$$\frac{\lambda}{n_i + n_i \sin\theta_i} \le P. \tag{4}$$

As it is easier to fabricate large structures, the largest period avoiding any presence of orders in the 3-5 µm region has to be found. To be a little less exigent, we will consider the 3.4-5 µm. This is not so dramatic in the sense that the atmospheric transmission becomes significant only above 3.4 µm. In this range of wavelengths, the refractive index of silicon is 3.42. Thus at normal incidence, the period of the grating has to be smaller than 1 µm. As shown in Fig. 4, Fourier Modal Method calculations allows us to determine for flat-top pyramids [Fig. 1(a)] of 1 and 1.3 µm period gratings, the efficiency of each order present in the incident medium. Parameters M and T are fixed (0.375 and 1.57 µm respectively). It may be observable that for each structure, [1, 0] and [-1, 0] modes have a strong efficiency when compared to the specular reflection [0, 0]. As predicted by the gratings formulae, these modes disappear for wavelengths around 1 and 1.3 µm for the 1 µm and 1.3 µm period gratings respectively. Furthermore, it is also observable that [2, 0] and [-2, 0] modes have a non-negligible value for both structures. For the 1.3 µm period grating, even [3, 0] and [-3, 0] orders are noticeable. Although P = 1.3 µm grating provides a slightly lower overall reflectance in the visible region, we want to limit the number of diffracted orders in order to avoid any trouble in the imaging systems. Thus we will restrain ourselves to periods smaller or equal than 1 µm only.

#190203 - $15.00 USD Received 8 May 2013; revised 15 Jun 2013; accepted 24 Jun 2013; published 27 Jun 2013

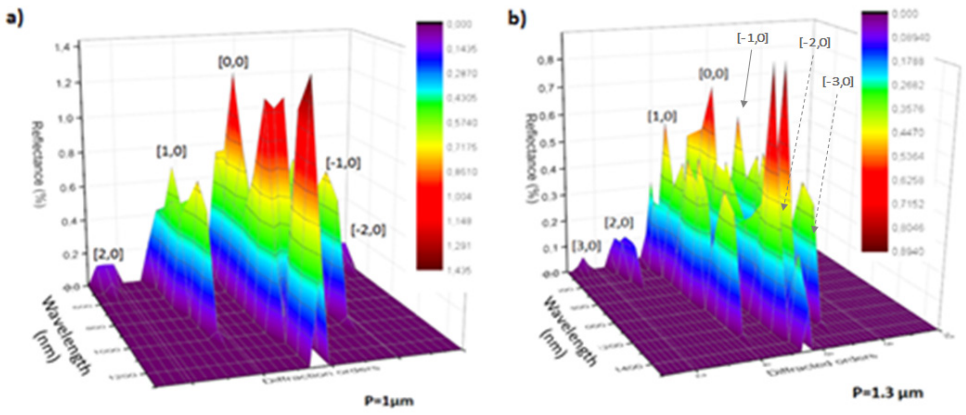

Fig. 4. 3D mapping of the diffracted orders efficiency in the incident medium versus the wavelength for flat-top pyramids grating of 1 µm (a) and 1.3 µm (b) period at normal incidence.

2.2.2 Variation in the period length

In order to understand the effect of a variation of the period length, FDTD calculations have been carried out. Parameters M and T are fixed (0.375 and 1.57 µm respectively) and the period P is varied from 0.7 to 1.3 µm. The reflectance spectrum is depicted in Fig. 5 and Table 1 reports the value of the θ angle for different P parameters.

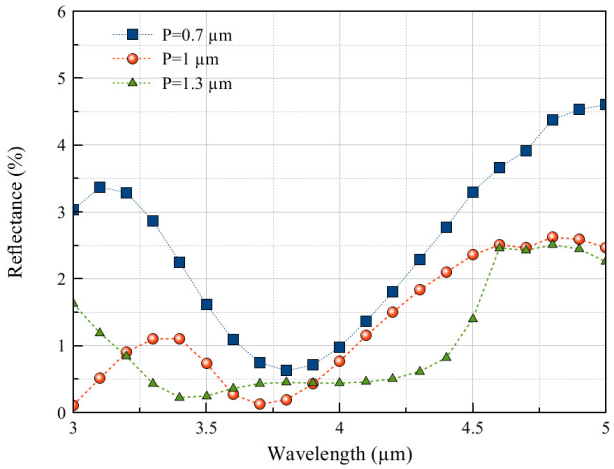

Fig. 5. Reflectance spectrum at normal incidence of a flat-top pyramid grating with T = 1.57 µm, M = 0.375 µm and s = 0 µm. The parameter P is varied from 0.7 to 1.3 µm.

Table 1. θ value for a grating with different length period P, and with M = 0.375 µm, T = 1.5 µm and s = 0 µm.

P (µm)	0.7	1	1.3
θ (°)	84.1	78.7	73.5

The structures with period P = 0.7 µm is too reflective in the 3-5 µm and will not be retained. For structures with periods P = 1 µm and P = 1.3 µm, the reflection coefficient is less than 2% in the 3-5 µm region. The latter one, with a slope angle of 73.5 °, shows the lowest reflectivity. However, as we want to restrain the efficiency of the diffracted orders (see section 2.2.1), we do not retain either of the structures with a period P = 1.3 µm.

#190203 - $15.00 USD Received 8 May 2013; revised 15 Jun 2013; accepted 24 Jun 2013; published 27 Jun 2013

2.2.3 Variation of the thickness

The M and P parameters are fixed (0.375 µm and 1 µm respectively) while the thickness T is varied. The reflectance spectrum is depicted in Fig. 6 and Table 2 reports the values of the angle θ for different T.

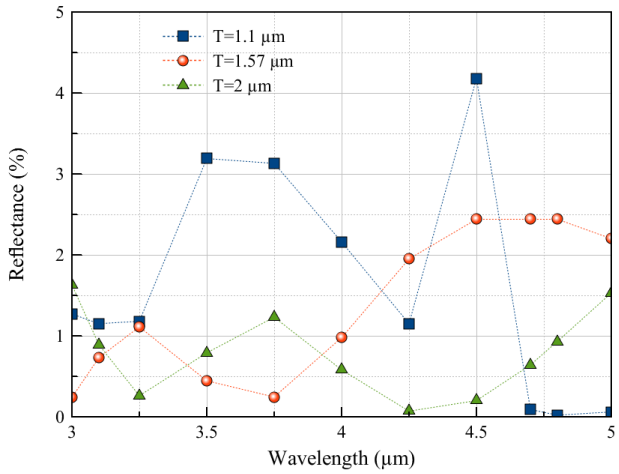

Fig. 6. Reflectance spectrum at normal incidence of a flat-top pyramid grating with P = 1 µm, M = 0.375 µm and s = 0 µm. The parameter T is varied from 1.1 to 2 µm.

Table 2. θ value for a grating with different thicknesses T, and with P = 1 µm, M = 0.375 µm and s = 0 µm.

T (µm)	1.1	1.57	2
θ (°)	74.1	78.7	81.1

It can be observed that the slope has a minor effect compared to the height of the pyramid. Indeed, the best efficiency is achieved for a 2 µm flat-top pyramid, showing a slope of the order of 81°. In terms of height, a too small pyramid (1.1 µm) cannot yield less than 2% reflectivity. On the other hand, objectives are achieved with structures with T = 1.57 µm and higher.

2.2.4 Variation in the flat-top length

Figure 7 gives the reflectance of three structures with the following parameters: P = 1 µm, T = 1.57 µm and s = 0 µm. M is equal to 0.1, 0.375 or 0.6 µm.

#190203 - $15.00 USD Received 8 May 2013; revised 15 Jun 2013; accepted 24 Jun 2013; published 27 Jun 2013

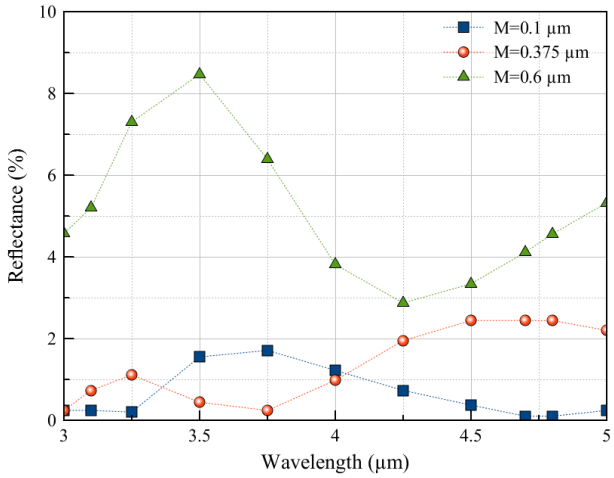

Fig. 7. Reflectance spectrum at normal incidence of a flat-top pyramid grating with T = 1.57 µm, P = 1 µm and s = 0 µm. The parameter M is varied from 0.1 to 0.6 µm.

Table 3 reports the value of the angle θ for different M value.

Table 3. θ value for a grating with different length of the flat-top M, and with P = 1 µm, T = 1.5 µm and s = 0 µm.

M (µm)	0	0.1	0.2	0.375	0.6
θ (°)	72.2	73.9	75.6	78.7	82.7

It can be observed that a 10° change in the slope can have a dramatic influence on the efficiency of the grating. The best efficiency is obtained for a slope angle of 73.9°. Structures having a flat-top smaller than 0.4 µm will demonstrate an average reflectivity coefficient R less than 2% in the 3-5 µm region. Structures with larger flat-top will then not be acceptable. It can be seen as well, that the best efficiency is achieved with M = 0.1 µm. However, structures with a flat-top smaller than 0.2 µm are hard to fabricate (see section 3.1).

2.2.5 Variation of the spacing

Simulations have been made to determine how much the spacing "s" at the bottom end of the structures [Fig. 8(a)] would be detrimental to the efficiency of the grating [Fig. 8(b)]. The parameters used are those of the reference structure: P = 1 µm, T = 1.57 µm and M = 0.375 µm. The spacing s is varied from 0 to 1 µm. Results show that, as expected, even a small spacing of 0.2 µm is sufficient to increase the average reflectivity to a value higher than 2%. Therefore, gratings with spacing between the structures will not be accepted.

#190203 - $15.00 USD Received 8 May 2013; revised 15 Jun 2013; accepted 24 Jun 2013; published 27 Jun 2013

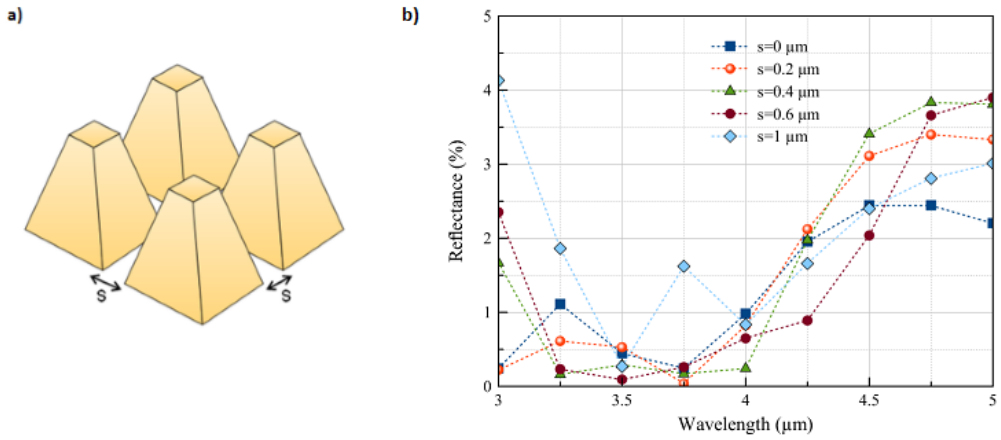

Fig. 8. Schematic view of the spacing between the structures (a) and reflectance spectra at normal incidence of flat -top pyramid grating with P = 1 µm, M = 0.375 µm and T = 1.5 µm. The spacing s is varied from 0 to 1 µm (b).

2.2.6 Geometrical specifications

This study has permitted us to define realistic parameters for the flat-top grating, in order to fabricate efficient antireflective silicon gratings. A set of parameters has been fixed. For less than 2% reflectance in the 3-5 µm region, the retained flat-top pyramids have to show the following parameters:

- Length of the flat-top M: 0.2-0.4 µm
- Length of the period P: 1 µm
- Thickness of the pyramid T: greater than 1.57 µm
- Slope must be comprised between 70 and 80 °
- No spacing between the structures

Also, the fabrication of a patterned-topped pyramid is considered as well. With the aim of broadening the antireflective range down to the visible region, adding another flat-top pyramidal pattern on top of a classical flat-top pyramid allows to demonstrate two antireflective bands. While the first level is efficient for the 3-5 µm wavelength range, by scaling down the geometric parameters of the second level of periodicity following a ratio of M/2P, it is possible to decrease the reflection in the visible region [Fig. 9]. Therefore the parameters of the second level are: $p = M/2P \times P$, $t = M/2P \times T$ and $M = M/2P \times M$ (see Fig. 1(b)). As the second level of periodicity is proportional to the first one, geometric specifications detailed above are still valid for the patterned-topped structures.

#190203 - $15.00 USD Received 8 May 2013; revised 15 Jun 2013; accepted 24 Jun 2013; published 27 Jun 2013

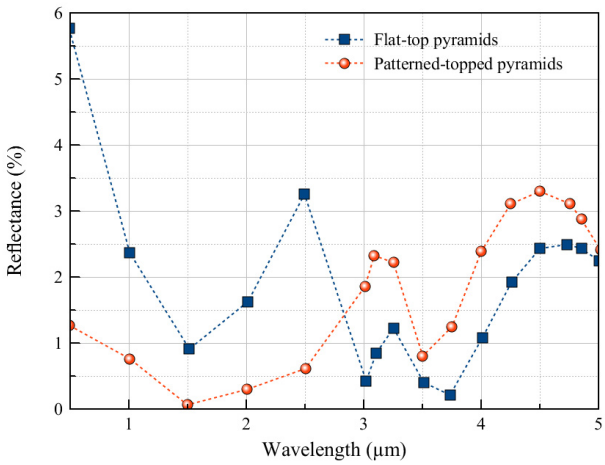

Fig. 9. Calculated reflectance spectra at normal incidence of flat-top and patterned-topped pyramids. Parameters of the flat-top pyramids are P = 1 µm, M = 0.375 µm, T = 1.5625 µm and spacing s = 0 µm. Parameters of the patterned-topped pyramids' first level are P = 1 µm, T = 1.25 µm and M = 0.5 µm. Parameters of the second level are p = 0.25 µm, t = 0.3125 µm, m = 0.125 µm.

3. Fabrication

After setting the parameter range necessary to achieve an efficient antireflective grating, several samples have been fabricated by plasma etching on a silicon surface. However, as it has not been possible to fabricate a silicon flat-top pyramids grating, a flat-top cone one was made instead. In this section, the fabrication process is first described, then a discussion will be dedicated to the fabricated samples.

3.1 Process

The flat-top cones were fabricated using DeepUV lithography and plasma etching processes. The photoresist was exposed with a 248 nm laser beam of a DUV stepper on 200 mm silicon wafers in order to define 300 nm dots. Nominal features are squares but since their dimension is close to the equipment resolution, circular structures have been obtained. The transfer into silicon was performed through a 100 nm thick SiO2 hardmask with a Centura 300 plasma etching cluster from Applied Materials. A specific etching process was developed to control the cone slope with high accuracy from 70° to 80°. Moreover this patented process allows a perfect control of the sharp profile at the bottom of the patterns. It has been demonstrated that this process is reproducible. The patterned-topped cones were fabricated by e-beam lithography and the same plasma etching processes. The main advantage of this process is that the cones exhibit no spaces and a sharp profile at the bottom of the features for both structuration levels. Once again this process is reproducible and geometrical parameters can be controlled with the top cone diameter defined by E-beam lithography.

3.2 Fabricated samples

Figures 10(a) and 10(b) present flat-top cones and patterned-topped cones respectively, characterized using Scanning Electron Microscopy. The patterns dimensions are listed: M = 310 nm, P = 1 µm and T = 1.6 µm for flat-top patterns and m = 125 nm, t = 325 nm, p = 250 nm, M = 500 nm, T = 1.25 µm and P = 1 µm for patterned-topped cones.

#190203 - $15.00 USD Received 8 May 2013; revised 15 Jun 2013; accepted 24 Jun 2013; published 27 Jun 2013

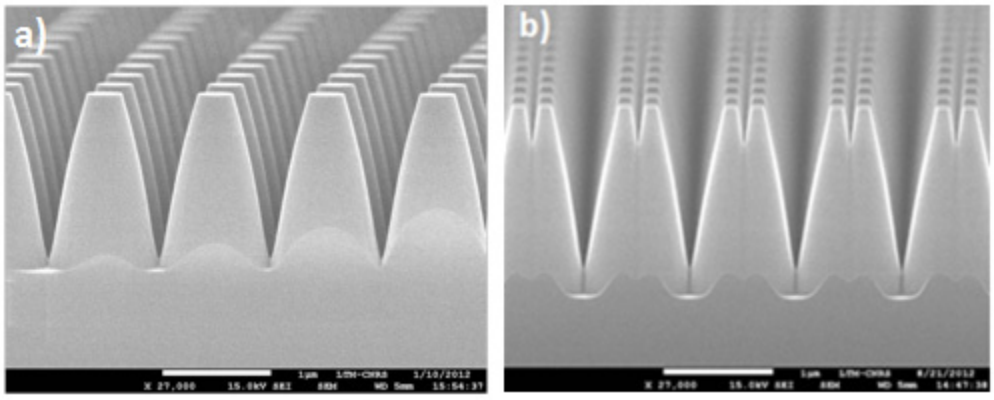

Fig. 10. SEM picture of flat-topped (a) and patterned-topped (b) silicon cones gratings.

Figure 11(a) shows that for the same P, M and T parameters, a flat-top cone grating is roughly 1% less efficient as an antireflective grating than a pyramid one. This is mostly due to the fact that the cone structures are not totally joined (as it has been seen for the pyramids grating), letting appear a small flat surface contributing to increase the reflectivity [Fig. 11(b)]. Although the first simulations were meant for pyramids, we decided to keep the same geometrical specifications for the cone grating.

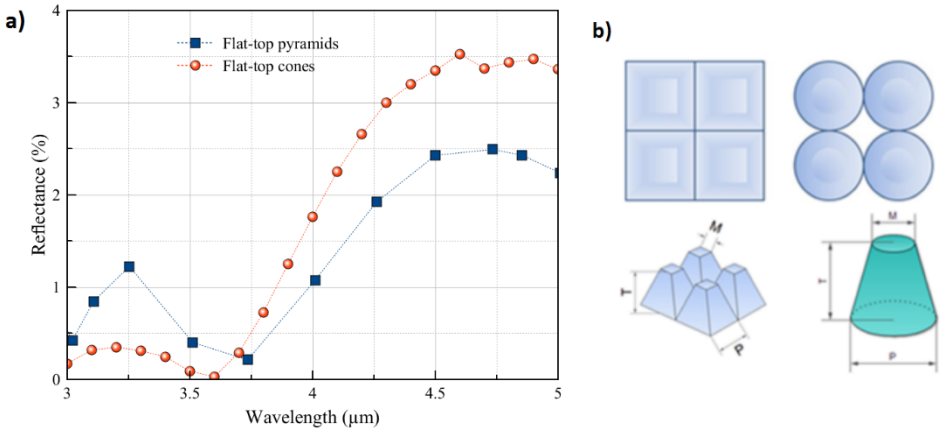

Fig. 11. Calculated reflectance spectra at normal incidence of a flat-top pyramid and a flat-top cone grating with P = 1 µm, T = 1.5 µm, M = 0.375 µm and s = 0 µm (a), schematic top view of flat-top pyramid and cone gratings and their parameters (b).

4. Optical measurements

Performances of the fabricated samples in the visible and mid infrared regions have been measured with an integrating sphere and a Fourier Transform Infrared (FTIR) spectrometer. In the first place, the reflectance of the flat-top cone gratings has been measured in the 3-5 µm region. Following the good results, patterned-topped cone gratings have been fabricated. From there, a comparison of the optical responses in the visible and mid infrared regions with the two types of gratings has been made.

4.1 Flat-top cones gratings

Most of the samples present M and P parameters close to those specified (around 0.32 and 1 µm for M and P parameters respectively). The height T of the flat-top cone is rather variable and goes from 1.21 up to 1.97 µm. Some of the samples present no spacing between the

#190203 - $15.00 USD Received 8 May 2013; revised 15 Jun 2013; accepted 24 Jun 2013; published 27 Jun 2013

structures. Geometric parameters of the series of samples are reported in Table 4. FTIR measurements are depicted in Fig. 12.

Table 4. Parameters of the fabricated flat top cone gratings

Sample	G23	G25	G30	G31	G37	G39
θ (°)	76,4	77,2	77,7	79,5	79,8	79,7
M (µm)	0.319	0.330	0.319	0.330	0.320	0.320
P (µm)	0.941	1.000	1.010	1.010	1.030	0.980
T (µm)	1.290	1.480	1.590	1.840	1.970	1.820
s (nm)	90	30	0	0	0	0

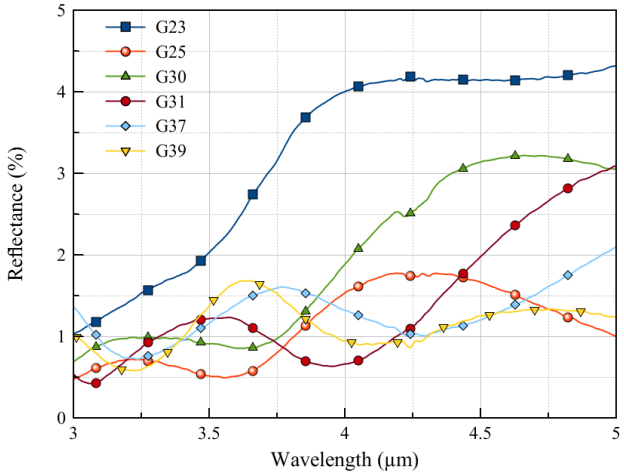

Fig. 12. Reflectance measurements of the fabricated silicon flat-top cone gratings.

As expected, the structuration strongly decreased the reflectivity when compared to a polished silicon surface (R = 30% in the 3-5 µm region). Best performances are then obtained by samples showing small or even zero spaces between the structures and high thicknesses (samples G25, G31, G37 and G39). Those samples demonstrate an average reflection coefficient less than 2% in the 3-5 µm region. The performances displayed are satisfying since we are considering flat-top cone gratings.

4.1 Extending the antireflective properties to the visible

After having successfully demonstrated a less than 2% reflectivity in the mid infrared with flat-top cone gratings, elaboration of patterned-topped cone gratings have been carried out (see section 3). As described in section 2.2.6, the patterning of the top of the cones has the goal of extending the antireflective properties up to the visible band.

#190203 - $15.00 USD Received 8 May 2013; revised 15 Jun 2013; accepted 24 Jun 2013; published 27 Jun 2013

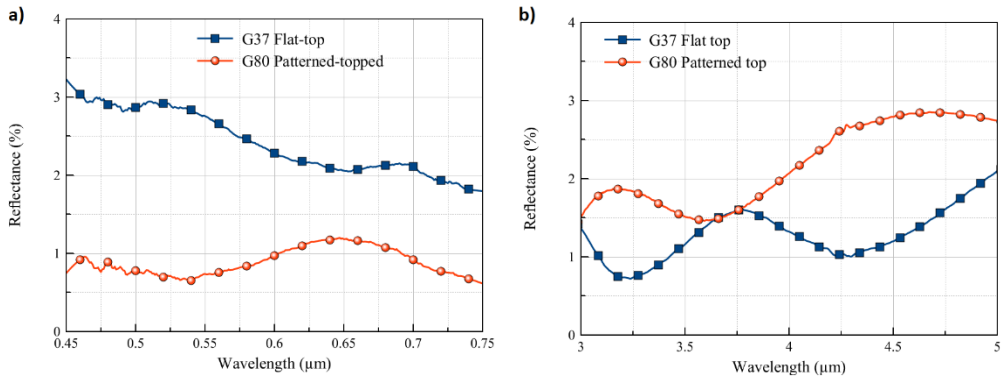

Fig. 13. Reflectance spectra of flat-and patterned-topped cones gratings measured in the visible by integrating sphere (a) and in Infrared by FTIR spectrometry (b).

Integrating sphere measurements [Fig. 13(a)] clearly shows that, due to the second periodicity level, the reflectivity of the patterned-topped cone (named G80 here, parameters are P = 967 nm, T = 1.368 µm and M = 502 nm for the first level, p = 251 nm, t = 342 nm and m = 119 nm for the second level) in the visible region has been lowered. However, as the index profile has been changed by patterning the top of the cones, performances of the patterned-topped structures have been slightly degraded as well in the 3-5 µm range [Fig. 13(b)] as it has already been demonstrated in another regime of wavelength [20]. Nonetheless those results are very promising and with a little more optimization, improvements in the mid infrared are yet to be expected.

5. Conclusion

Investigations on periodically structured silicon surfaces have been performed. The main objective was to demonstrate an antireflective coating with less than 2% reflectance for the 0.45-0.75 µm and 3-5 µm wavelength bands. Definitions of realistic parameters for the flat-top grating have been made through FDTD and Modal Fourier Method calculations in order to fabricate efficient antireflective silicon gratings. A set of parameters has then been fixed. Performances of the fabricated samples have then been measured by Fourier Transform Infrared Spectrometry. Best performances have been obtained by samples showing no spaces between the structures and high thicknesses, demonstrating an average reflectance smaller than 2% in the 3-5 µm wavelength range. Finally, in order to extend the AR band up to the visible region, patterned-topped cones have been fabricated. Even though performances in the mid infrared range have been slightly deteriorated, optical measurements show a clear enhancement of the AR efficiency in the visible region. With better optimization, even better results are to be expected and we may consider adding a third level of periodicity in order to extend the AR band a little more.

#190203 - $15.00 USD Received 8 May 2013; revised 15 Jun 2013; accepted 24 Jun 2013; published 27 Jun 2013